ORO/5217-5

MACRO-ENCAPSULATION OF PCM

QUARTERLY REPORT
OCTOBER 1977 TO DECEMBER 1977
CONTRACT E (40-1)-5217

Prepared for
DOE
Oak Ridge, Tenn.

by
THE DOW CHEMICAL CO.
MIDLAND, MICHIGAN 48640

DISCLAIMER

ATTACHMENT A

BIBLIOGRAPHIC DATA SHEET	1. Report No. ORO-5217-5	2.	3. Recipient's Accession No.

4. Title and Subtitle
Macro-Encapsulation of Heat Storage Phase Change Materials

5. Report Date
March 1977

6.

7. Author(s)
G. A. Lane, G. L. Warner, P. B. Hartwick, H. E. Rossow

8. Performing Organization Rept. No.

9. Performing Organization Name and Address
The Dow Chemical Company
Midland, MI 48640

10. Project/Task/Work Unit No.

11. Contract/Grant No.
E(40-1)-5217

12. Sponsoring Organization Name and Address
DOE, Oak Ridge, Tennessee 37830

13. Type of Report & Period Covered
Quarterly Report
Sept. 29, 1977-Dec. 29, 1977

14.

15. Supplementary Notes

16. Abstracts
Objectives are to assess the feasibility of macro-encapsulated PCM's for residential solar systems, to develop and evaluate such materials. Encapsulant materials under consideration are multilayer flexible plastic films, steel cans, and plastic bottles. PCM's under study are $Mg(NO_3)_2 \cdot 6H_2O$, stearic acid, $Mg(NO_3)_2 \cdot 6H_2O$-NH_4NO_3. A study of the storage capability of $CaCl_2 \cdot 6H_2O$ encapsulated in polyethylene bottles has been completed.

17. Key Words and Document Analysis. 17a. Descriptors
Solar Energy
Heat Storage
Phase Change Materials
Heat-of-Fusion
Isothermal Storage
Encapsulation

17b. Identifiers/Open-Ended Terms
Storage of Solar Heat
Isothermal Phase-Change Heat Storage
Encapsulation of Heat Storage Materials

17c. COSATI Field/Group

18. Availability Statement	19. Security Class (This Report) UNCLASSIFIED	21. No. of Pages
	20. Security Class (This Page UNCLASSIFIED	22. Price

ORO/5217/5
UC94a

MACRO-ENCAPSULATION OF HEAT STORAGE PHASE-CHANGE MATERIALS for Use in Residential Buildings

Fifth Quarterly Progress Report

September 29, 1977 - December 29, 1977

by

George A. Lane

Greg L. Warner

Phillip B. Hartwick

Harold E. Rossow

The Dow Chemical Company

Midland, Michigan 48640

March 1978

Prepared for the United States
Department of Energy
Division of Energy Storage Systems

Contract E(40-1)-5217

TABLE OF CONTENTS

FOREWORD

The work described in this report is an extension of a basic effort already performed under contract NSF-C906. The general objectives are: 1) to assess the technical and economic feasibility of encapsulated phase change materials (PCM's) for storing heat in residential solar energy systems, and 2) to develop and evaluate such encapsulated phase change materials.

The project involves three tasks:

Task 1 - Materials selection, including a limited literature search, selection of candidate phase change materials, and selection and characterization of encapsulating materials.

Task 2 - Procurement of phase-change and encapsulating materials, encapsulation studies, and testing of the encapsulated materials.

Task 3 - Preliminary design and economic evaluation of a residence-sized heat storage sub-system.

Task 1 has been completed, and Task 2 efforts are in progress.

I. PHASE CHANGE MATERIALS

Evaluation of $CaCl_2 \cdot 6H_2O$ in high density polyethylene bottles has been completed. This report will be mainly a review of these data. The next material to be evaluated will be $Mg(NO_3)_2 \cdot 6H_2O$ encapsulated in steel aerosol cans.

Further data on thermal conductivity of PCM's are shown in Figure 1. In the liquid range, $Mg(NO_3)_2 \cdot 6H_2O$ and its eutectic with NH_4NO_3 have about the same thermal conductivity. The naphthalene-benzoic acid eutectic gives a value only about a fourth that of the salt hydrates.

II. ENCAPSULATED PCM'S

We have discovered that the effects of expansion and contraction during melting and freezing of PCM's has a more severe effect on the encapsulating medium than we anticipated. For example, after 66 cycles in the heat storage test device, about half of the polyethylene bottles showed signs of stress cracking. This is being investigated more fully and will be discussed in future reports.

III. TESTING PROCEDURES

ASHRAE (94-77) standards for testing thermal storage units were followed. All of these tests require that the temperature of the storage medium, prior to the start of the test time (τ), be uniform at the desired temperature with a steady flow of transfer fluid (air) through the storage unit (steady-state). The test time begins with a step change of 35°C in the inlet air stream. For a latent heat type storage unit, this 35°C step change must symmetrically bracket the fusion temperature, thereby forcing the storage medium to undergo a change of phase. Since the fusion temperature of $CaCl_2 \cdot 6H_2O$ is 27°C, the inlet air temperature will step change from

---

[1] American Society of Heating, Refrigeration, and Air Conditioning Engineers.

Figure 1

THERMAL CONDUCTIVITY VS. TEMPERATURE

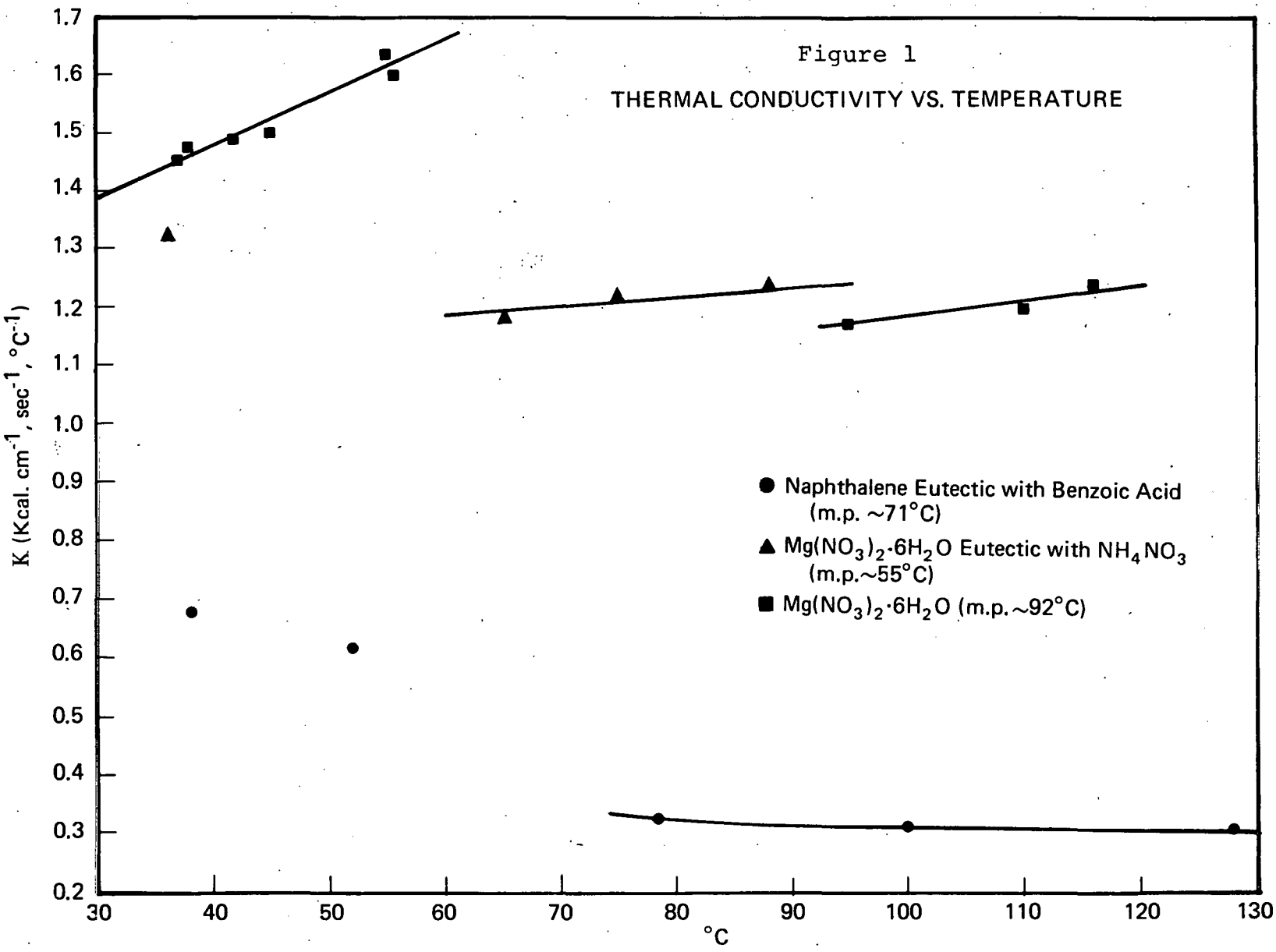

9.5°C to 44.5°C, where it is held constant while charging the unit. A temperature-time profile of the outlet temperature during charging is shown in Figure 2 for a nearly ideal latent heat storage unit. The test time ends when the outlet temperature reaches midway between the inlet and fusion temperatures, defined as the "maximum charge temperature" (35.75°C). The charge design rate is set equal to this minimum useful charge rate. Following attainment of steady-state conditions the inlet temperature is step changed from 44.5°C to 9.5°C where it is held constant to generate a discharge profile of the outlet temperature. Like the charging cycle, the test time ends when the outlet temperature reaches midway between the inlet and fusion temperatures defined as the "minimum discharge temperature" (18.25°C). The discharge design rate is set equal to this minimum useful discharge rate.

The areas between the inlet and outlet temperature profiles over the test times of charging (τ_c) and discharging (τ_d) are used to determine the charge and discharge capacities, CC and DC respectively, using the following equations:[1]

$$CC = \dot{m}\, C_{tf} \int_o^{\tau_c} (T_{in} - T_{out})\, d\tau - L \int_o^{\tau_c} \left(\frac{T_{in}+T_{out}}{2} - \bar{T}_a\right) d\tau \quad (1)$$

$$DC = \dot{m}\, C_{tf} \int_o^{\tau_d} (T_{out} - T_{in})\, d\tau \quad (2)$$

The later half of equation (1) is simply the heat loss from the storage unit which is incurred during the charging cycle. This heat loss factor, a modified form of the equation given in ASHRAE standards, is more accurate since it doesn't assume a constant average temperature driving force between the storage unit and ambient air temperatures ($\bar{T}_{unit}-\bar{T}_a$). However, the heat loss rate constant (L) is determined from the equation given by the ASHRAE standards as follows:

---

[1] See p. 25 for nomenclature.

Figure 2

LATENT HEAT TYPE THERMAL STORAGE UNIT

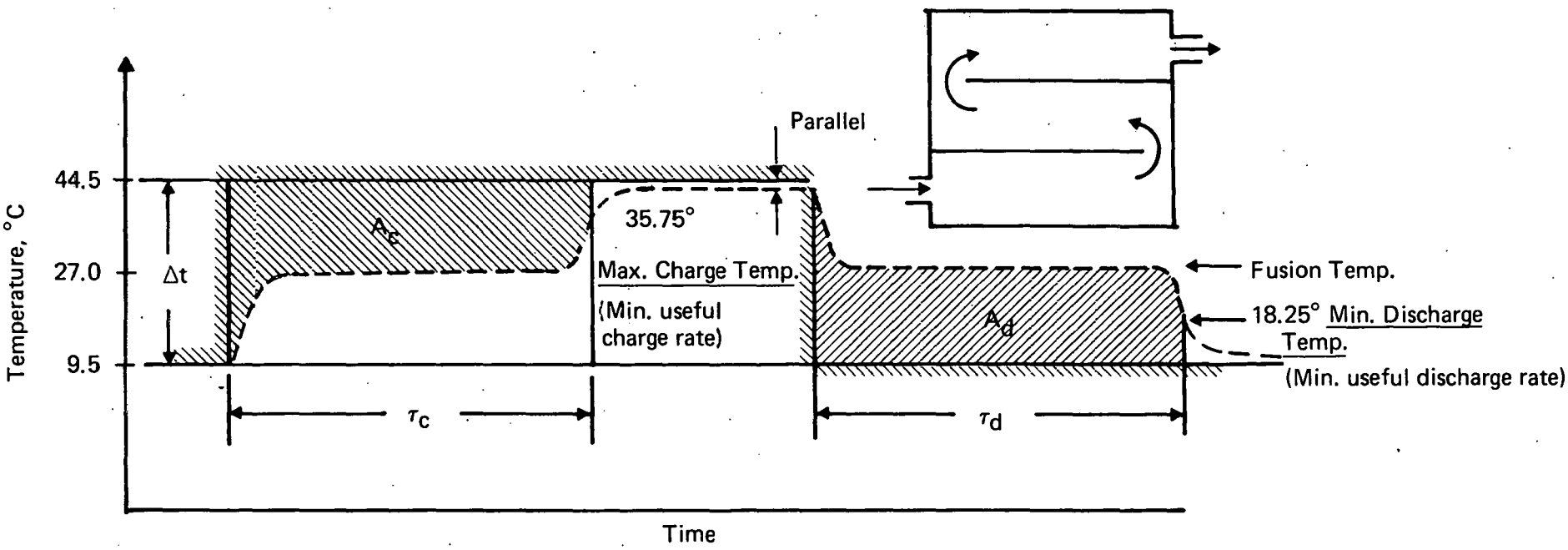

t_{in}, Inlet Temperature

t_{out}, Outlet Temperature

$CC = \dot{m}C_{tf}\ A_c$ - Loss = Charge Capacity

$DC = \dot{m}C_{tf}\ A_d$ = Discharge Capacity

$\dot{m}$ = Mass Flow Rate
C_{tf} = Specific Heat
} of Transfer Fluid (Air)

τ_c = Charge Time

τ_d = Discharge Time

$$L = \frac{\dot{m}\, C_{tf}}{(3600\ \text{sec})(25°)} \int_{o}^{3600} (T_{in} - T_{out})\, d\tau \qquad (3)$$

The integration of the above equation is made over a one hour period after the unit has achieved uniform steady-state temperatures with the inlet air temperature being 25°C above the average ambient air temperature ($\bar{T}_a$).

IV. HEAT STORAGE TEST RESULTS

The thermal energy storage unit used is shown in Figure 3. Sixteen-ounce high density polyethylene bottles (129) were filled with melted $CaCl_2 \cdot 6H_2O$ to 95% of capacity and sealed before freezing. The bottles were placed in the storage unit in an equilateral triangular pitch arrangement. Thermocouples were placed in nine bottles located at various positions (1-9) in the storage unit so that temperature-time profiles for individual bottles of $CaCl_2 \cdot 6H_2O$ may be observed. The storage unit was sealed and cycled for 58 complete freeze/thaw cycles before any data were taken.

For a typical charge cycle (Figure 4), the bottle located nearest the inlet (1) has the shortest response time, quickly melting and achieving steady-state. The remaining bottles all melt similarly, each achieving complete melting and steady-state in succession, with the bottle furthest from the inlet (9) finishing last. One exception is that for the bottles at positions 6 and 7 the order of melting is reversed. The presence of the bend in the air flow path of the storage unit causes either short-circuiting or a difference in air heat transfer coefficients. The end of the test time (14.3 hours) is indicated when the outlet air temperature reaches the "maximum charge temperature". At this time, all of the $CaCl_2 \cdot 6H_2O$ has melted except for a small portion of a few bottles at position 9. Since the

Figure 3

Calcium Chloride Hexahydrate Storage Medium,
Air - Heat Transfer Fluid, Thermal Energy Storage Unit

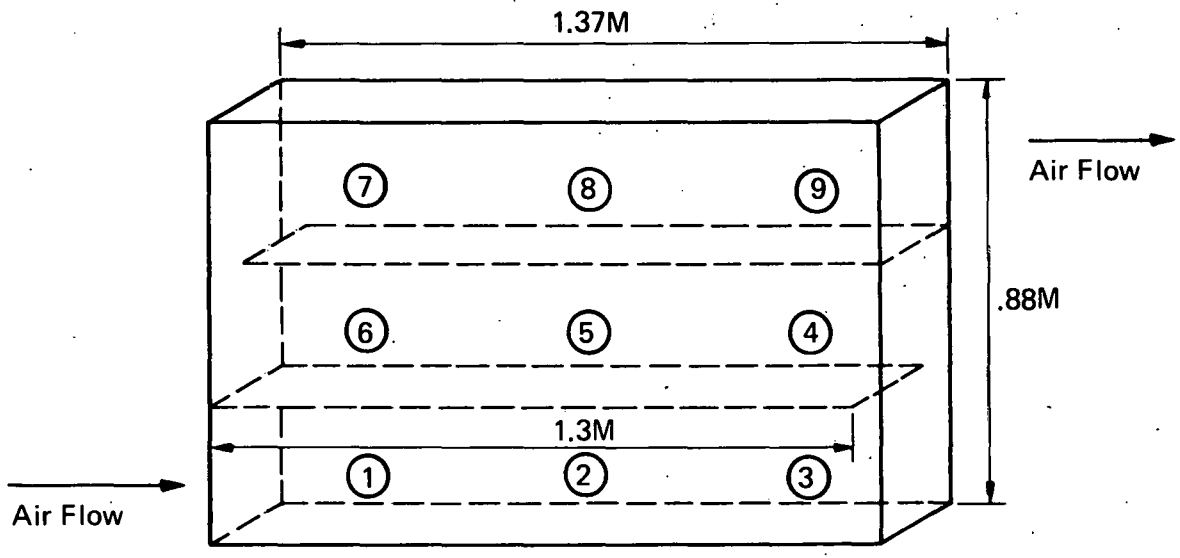

Cabinet 1/8" Steel - 125 Kg

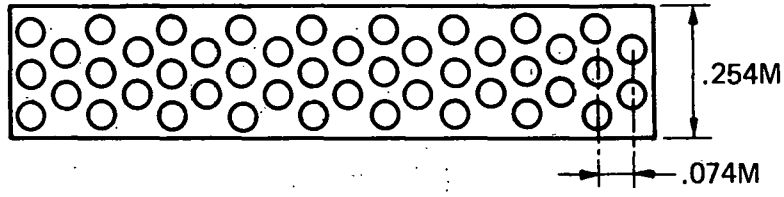

Containers .061M Dia .180 HT Bottles
Walls .74 mm HDPE

Layout .024M Spacing Equilateral Triangular Pitch
Minimum Possible Void Fraction .52
Bottle positions with thermocouples ① → ⑨

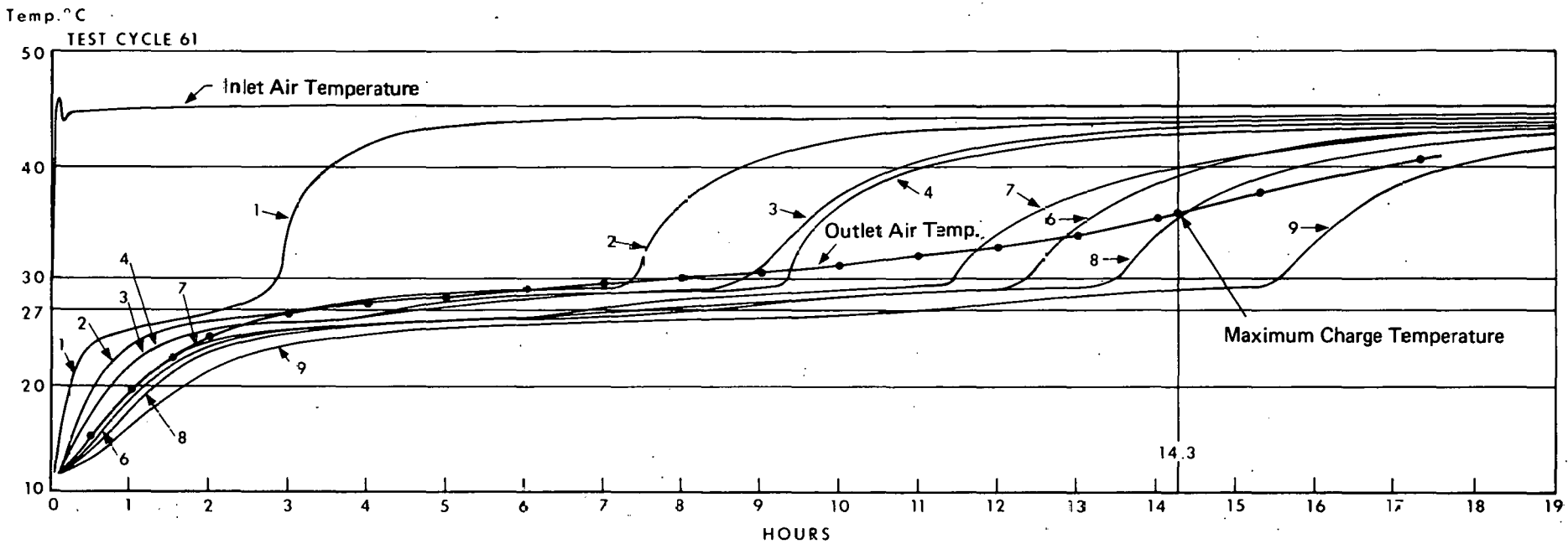

Figure 4: CHARGE CYCLE: Calcium Chloride Hexahydrate In HDPE Bottles

thermocouples are located at the center of the bottle, they measure the temperature of the last portion of material to melt. Thus, it is believed that the bottles are nearly all charged, and the small amount still frozen shouldn't significantly decrease the charge capacity.

A typical discharge cycle (Figure 5) shows similar successive trend curves for each bottle position, this time for cooling, with curves for positions 3 and 4 reversed as well as for 6 and 7. The end of this test time (11.5 hours), when the outlet temperature reaches the "minimum discharge temperature", several of the bottles aren't completely discharged (frozen), decreasing the discharge capacity. However, as in the charging cycle, the magnitude of the amount of material failing to discharge is exaggerated, since the temperatures are of the material which is the last to freeze. Still, the unit appears not to have discharged to the extent that it had charged.

The temperature profiles for the discharge cycle indicate that some supercooling of the $CaCl_2 \cdot 6H_2O$ is taking place. A plot of the extent of supercooling vs. the bottle position in the storage unit for four air flow rates is shown by Figure 6. Supercooling ranges from about 7.5°C for bottle positions nearest the inlet (1) to about 2.0°C for bottle positions nearest the outlet (9). Each successive bottle position from the inlet shows a decrease in the amount of supercooling, except for anomalous positions 3, 4, 6, and 7. This increase in supercooling may be attributed to heat transfer variations caused by the presence of the bend in the storage unit as seen for the case of reverse cooling curves during discharging. Similarly, the slightly increased supercooling at position 9 may be attributed to the sudden

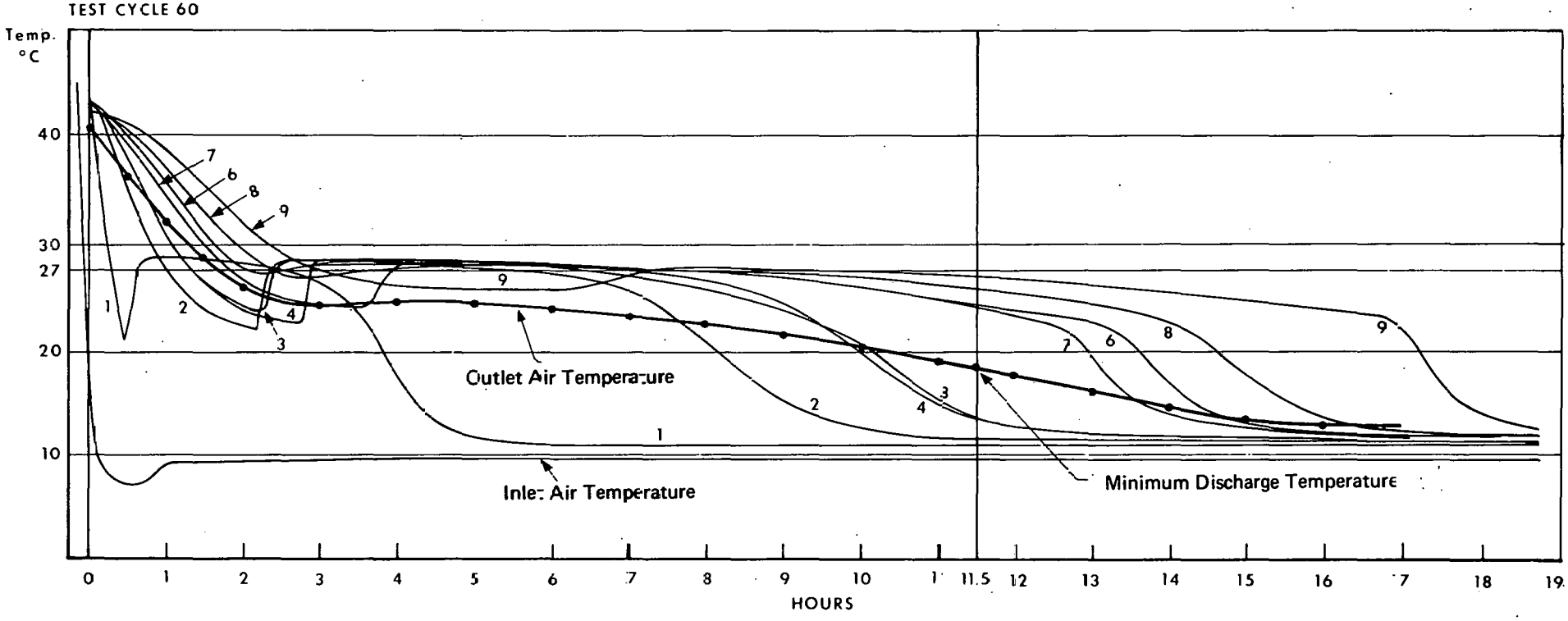

Figure 5: DISCHARGE CYCLE: Calcium Chlorice Hexahydrate In HDPE Bottles

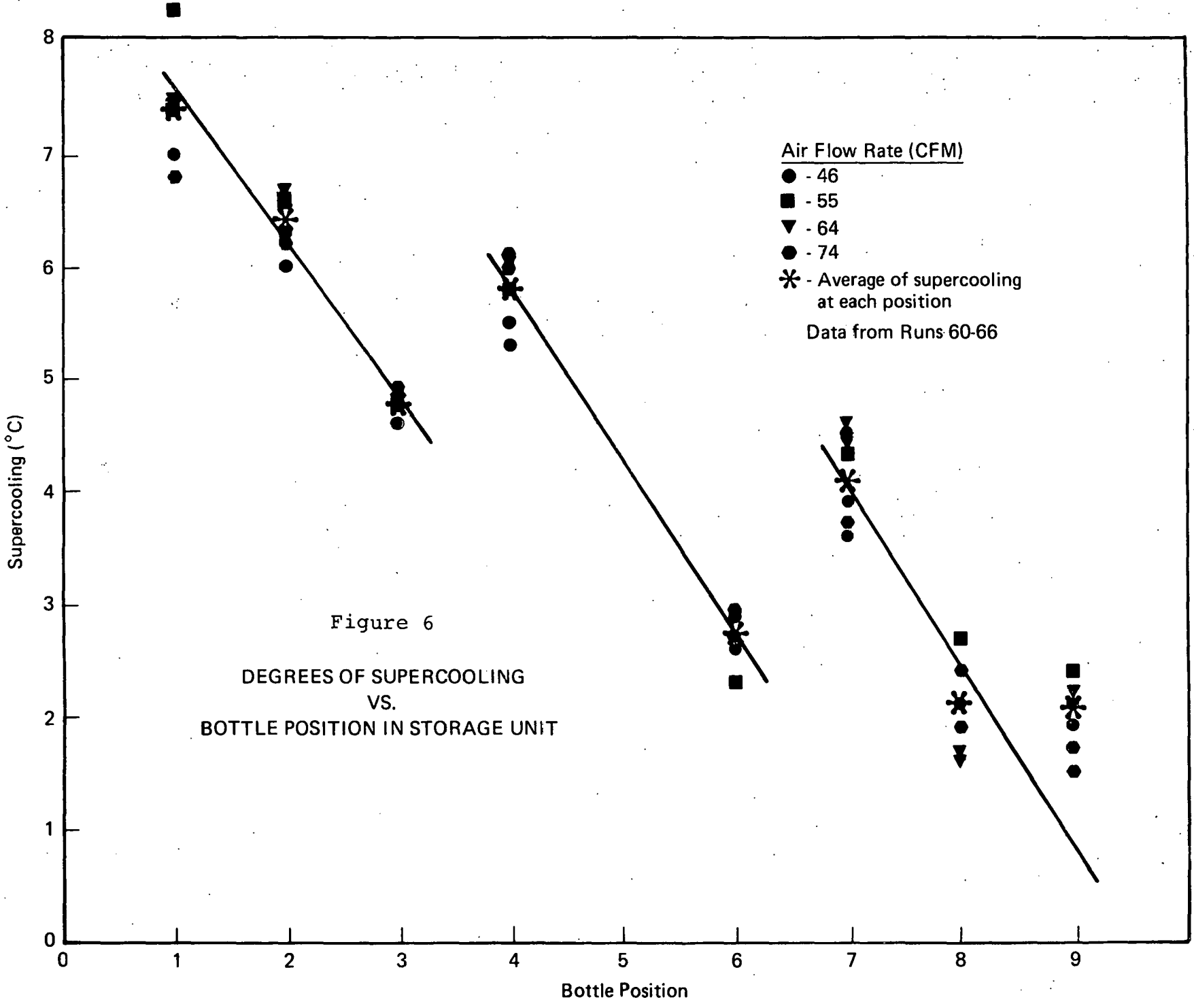

Figure 6

DEGREES OF SUPERCOOLING
VS.
BOTTLE POSITION IN STORAGE UNIT

contraction of the 11 1/2" x 10" rectangular conduit to a 4" diameter circular conduit. These variations in geometry throughout the unit may result in different rates of cooling, resulting in supercooling variations.

A total of eight pairs of charge/discharge cycles (Runs 59-66) were done at four air flow rates (46-75 CFM). Profiles of the outlet air temperature vs. time were generated according to the test procedures stated earlier, and are shown in Figures 7 and 8 for the charge and discharge cycles, respectively.

Even though each successive cycle was allowed to achieve steady-state before initiating the step change for the following cycle, the curves only show the profile generated for the time period of each test. As illustrated for the charging curve at 75 CFM (74 CFM for discharge), the shaded area between the inlet and outlet temperature profiles was manually integrated. As expected, the time necessary for charging (discharging) the unit increases as the air flow rate decreases. Note that the temperature profile obtained for the lowest air flow rate is most similar to that expected for the case of the nearly ideal latent heat type storage unit. This may be attributed to better equilibrium attainment of heat transfer through the PCM and heat transfer between the air and bottle surface. Also note that the net effect of supercooling and reheating is an increase of about 1/2°C observed during discharging.

The reduced data with energy balance results for runs 59-66 are shown by Table I. The runs of similar air flow rates have been grouped and arranged in decreasing order. Each heading, except the last, has subcolumns 1 and 2, representing the charge and discharge cycles, respectively.

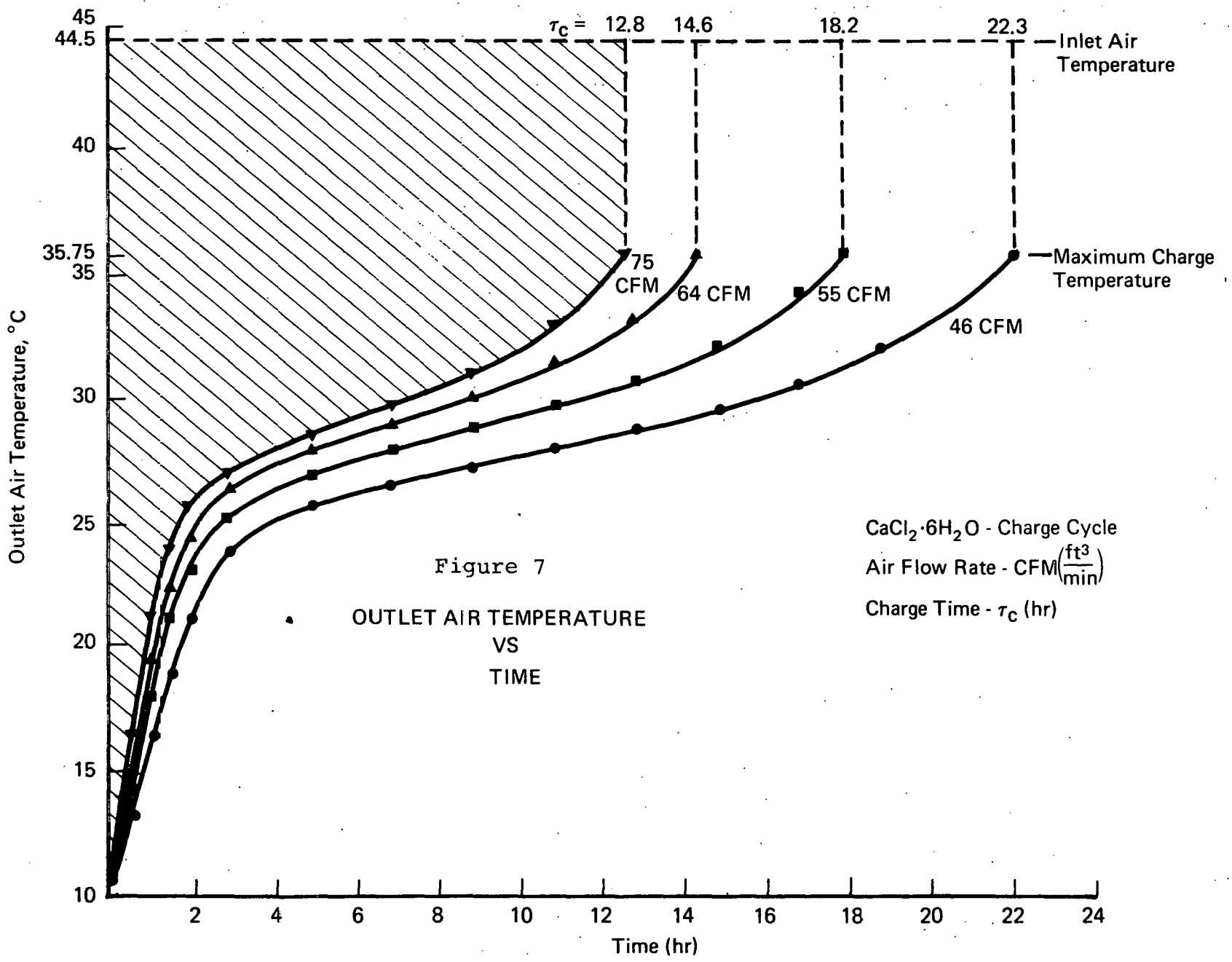

Figure 7

OUTLET AIR TEMPERATURE
VS
TIME

Figure 8

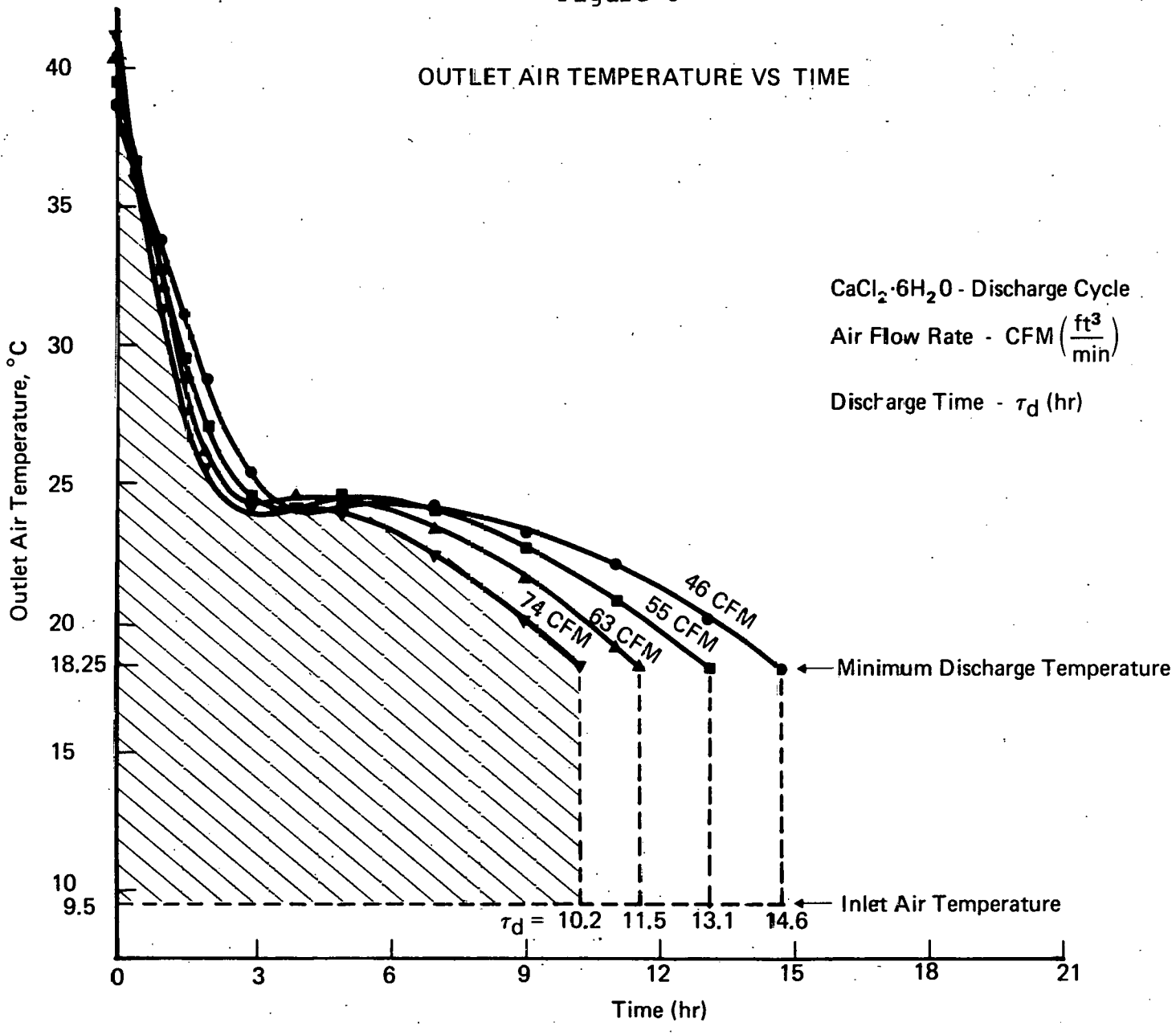
OUTLET AIR TEMPERATURE VS TIME
$CaCl_2 \cdot 6H_2O$ - Discharge Cycle
Air Flow Rate - CFM $\left(\frac{ft^3}{min}\right)$
Discharge Time - τ_d (hr)
Outlet Air Temperature, °C
40
35
30
25
20
18.25
15
10
9.5
46 CFM
55 CFM
63 CFM
74 CFM
Minimum Discharge Temperature
Inlet Air Temperature
τ_d = 10.2 11.5 13.1 14.6
0
3
6
9
12
15
18
21
Time (hr)

TABLE I: TEST RESULTS ON CALCIUM CHLORIDE HEXAHYDRATE ENCAPSULATED IN POLYETHYLENE BOTTLES

Run	Air Flow Rate (CFM) 1	2	Test Time (τ-Hr) 1	2	Storage Unit Pressure Drop (ΔP-in. H_2O) 1	2	Loss (KJ) 1	2	Capacity(KJ) CC (Q_{in}-loss) 1	DC (Q_{out}) 2	Energy Balance (KJ) (Q_{out}+loss)	% Dev
62	74	74	12.7	9.9	.42	.51	3,740	100	22,760	22,530	22,630	+0.6
63	75	73	12.8	10.2	.43	.50	4,130	160	22,770	22,790	22,950	-0.8
						Average	3,940	130	22,770	22,660	22,790	-0.1
59	64	65	14.6	11.0	.32	.40	4,300	480	22,920	23,000	23,480	-2.4
60	65	63	15.4	11.5	.33	.38	5,220	180	23,160	24,410	24,590	-6.2
61	63	62	14.3	12.0	.32	.38	4,010	80	22,630	23,310	23,390	-3.4
						Average	4,510	250	22,900	23,570	23,820	-4.0
64	55	55	18.2	13.1	.24	.29	5,650	410	22,980	22,540	22,950	+0.1
65	46	45	21.0	14.7	.17	.21	6,660	1,040	22,980	21,880	22,920	+0.3
66	46	46	22.3	14.6	.18	.22	6,950	160	24,350	22,470	22,630	+7.1
						Average	6,810	600	23,670	22,180	22,780	+3.8

1 = Charge

2 = Discharge

$$\% \text{ Dev} = \frac{(Q_{in}\text{-loss})-(Q_{out}\text{+loss})}{(Q_{in}\text{-loss})} \times 100$$

The results of the charge (discharge) times and the pressure drops across the storage unit are shown graphically as a function of the air flow rates in Figures 9 and 10. The test times varied from 13 to 22 hours for charging and 10 to 15 for discharging. The longer times for charging reflect the dominating effect of heat loss working against charging while working for discharging in attaining the final test temperatures. The discharge times are somewhat increased due to solid crystal build-up of the $CaCl_2 \cdot 6H_2O$ on the inside walls of the bottles, impeding heat transfer from the molten cores to the air. It is believed that this heat transfer limitation becomes a dominant factor for larger diameter bottles, resulting in a decreased storage capacity.

Theoretical pressure drop curves, derived from a relationship for air flow through a staggered arrangement of tube banks,[1] are shown in Figure 10. There are two curves because of the difference in density of the warm and cool air streams used during charging and discharging. There is good agreement between measured and predicted pressure drops for the range 0.2 to 0.5 inches of water. Decreasing the air flow rate yields a desirable low pressure drop, but increases the time needed to completely charge (discharge) a given capacity (KJ).

The heat loss during charging increases from about 3,900 KJ at 75 CFM to about 6,800 KJ at 46 CFM. The larger heat loss at lower air flow rates is due to the longer charge time. For the discharge cycle, heat loss shows a similar trend, but is minimal since the average temperature of the storage unit quickly drops below the ambient air temperature. For the energy balance, the loss during discharge is added to the discharge capacity and compared to the charge capacity. A % deviation, defined as the percent difference of this energy balance comparison relative to the charge capacity, is reported. With 0% deviation representing a perfect energy balance, the deviation is about $\pm$4%.

---

[1] Perry's Engineering Handbook; 4th Ed.; 5-47, 48 (1969).

Figure 9

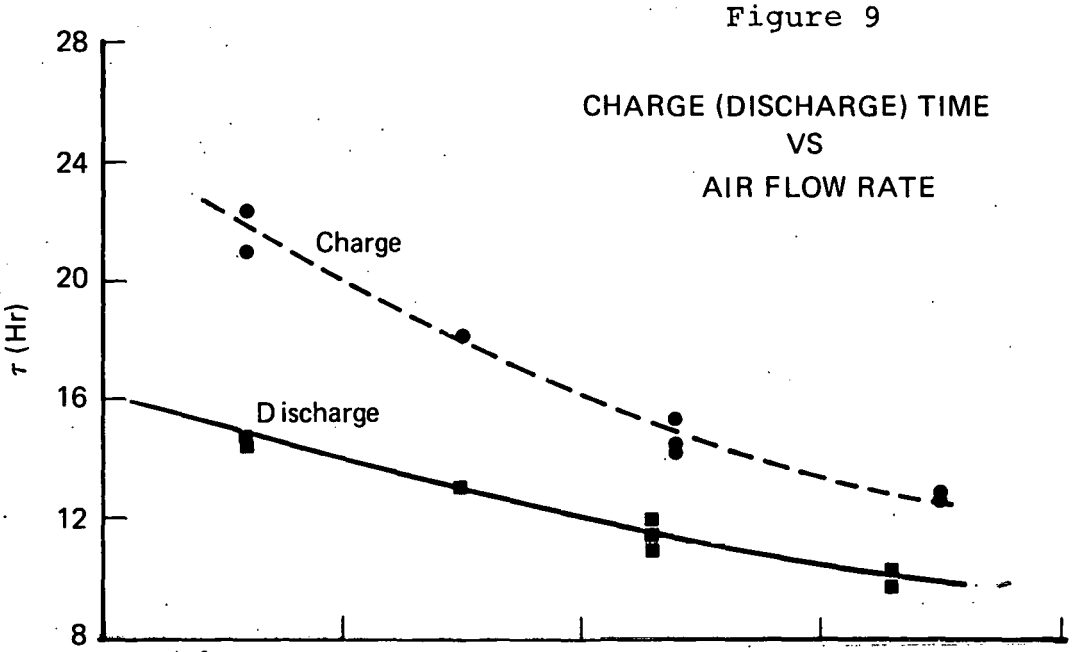

Figure 10

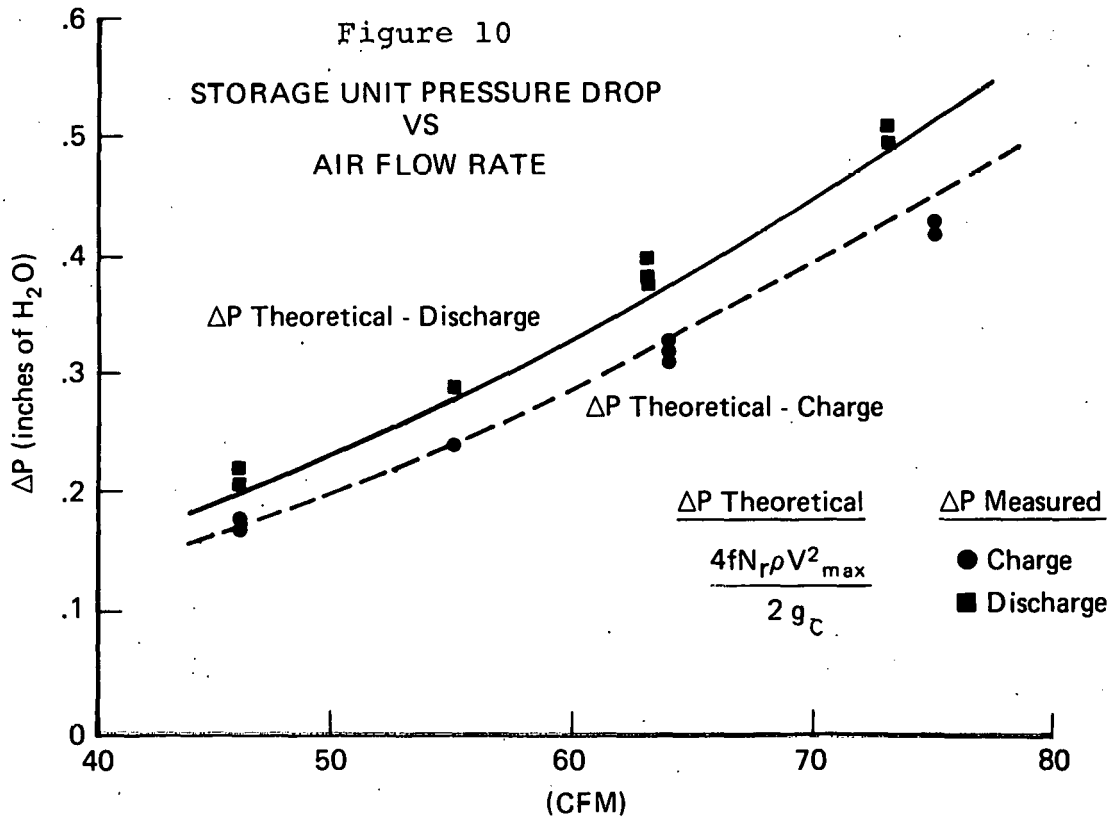

Theoretical charge and discharge capacities (TCC and TDC) are calculated for the storage unit with pertinent information and results listed in Table II. The temperature range of the

TABLE II

Theoretical Charge and Discharge Capacities

$CaCl_2 \cdot 6H_2O$		
Fusion Temp., °C	27	
Heat of Fusion, Cal/g	46	
Specific Heat, Cal/g°C	0.52 (liquid)	
	0.33 (solid)	
Total Weight, kg	97	
Steel (Storage Unit Structure)		
Specific Heat, Cal/g°C	0.10	
Total Weight, kg	125	
	Charging	Discharging
Temperature Range, °C		
High	35.75	44.50
Low	9.50	18.25
Theoretical Capacity, KJ[1]	24,190 (TCC)	24,860 (TDC)

[1] Not including specific heat of polyethylene bottle encapsulant.

storage unit during the test is estimated using the minimum and maximum outlet air temperatures.

The theoretical and measured capacities were plotted against the air flow rate (Figure 11). The measured charge capacity increases slightly with decreasing air flow rate as more time is available for bottle contents and air temperatures to equilibrate. The measured discharge capacity oscillates for an unknown reason. Each measured capacity was divided by its respective theoretical capacity and plotted as a percent capacity vs. the air flow rate (Figure 12). For the flow rates used, the storage unit was able to charge and discharge an average of 95.4% and 91.5%, respectively, of its theoretical capacities. The difference between the percent capacity for charge and discharge is consistent with the observations of the temperature-time profiles for individual bottles in the storage unit. The charging cycle showed nearly all bottles of material completely charged (thawed) while the discharge cycle showed several bottles not completely discharged (frozen) by the end of the respective test times.

An important design criterion for a thermal storage unit is the charging (discharging) heat rate. A simple heat rate equation for the transfer fluid may be expressed as follows:

$$q = \dot{m} C_{tf} \Delta T \qquad (4)$$

The values and results of this equation for runs 59-66 are shown in Table III. Again, the runs with similar air mass flow rates (kg/hr) are grouped and arranged in descending order. The pertinent inlet and outlet air temperatures for the charging and discharging cycles are shown at the bottom of the table. The charge (discharge) rate will be a maximum at the beginning, immediately following the step change of

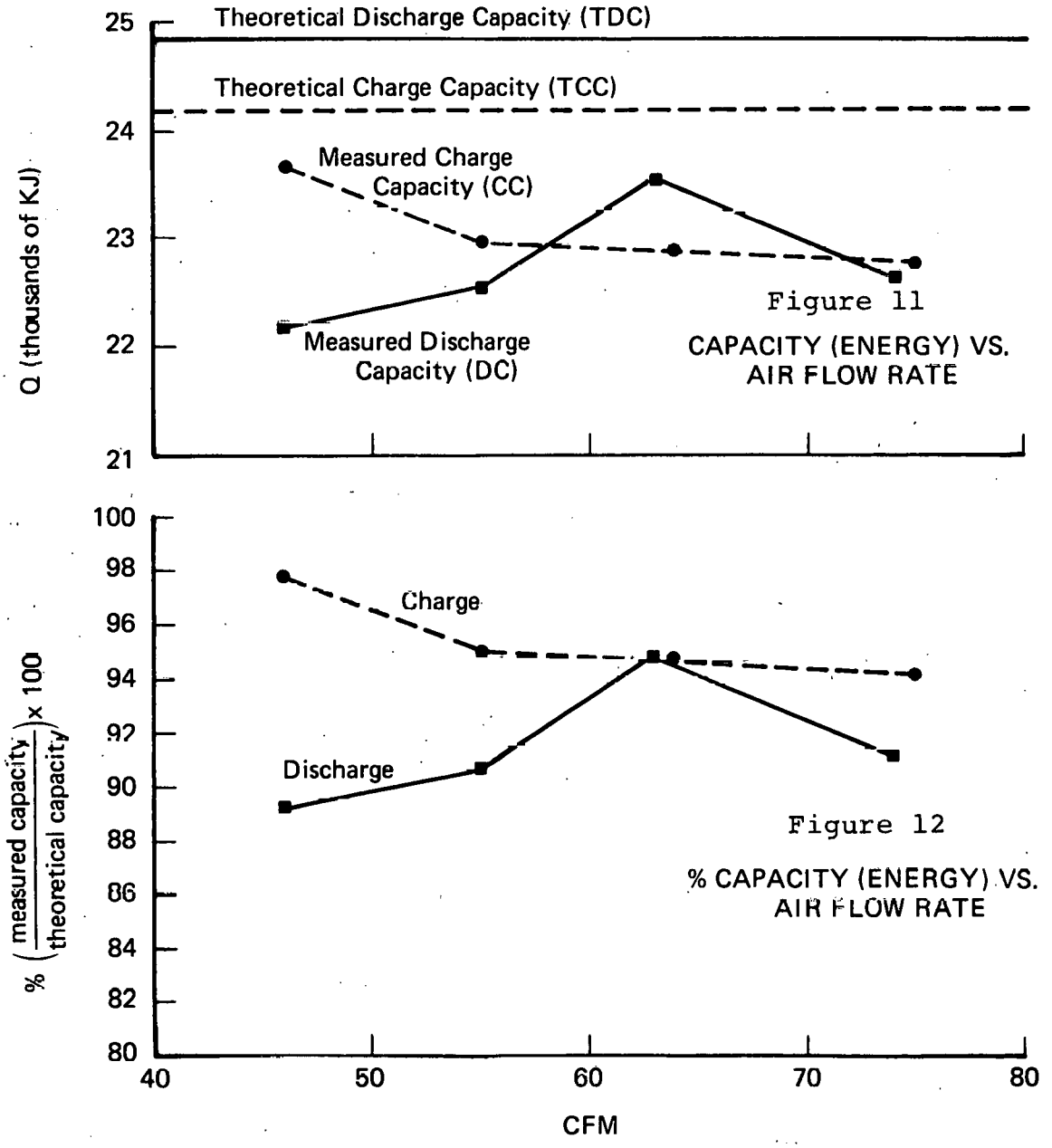

Figure 11

CAPACITY (ENERGY) VS. AIR FLOW RATE

Figure 12

% CAPACITY (ENERGY) VS. AIR FLOW RATE

TABLE III: CHARGING AND DISCHARGING HEAT RATE

Run	Air Mass Flow Rate ($\dot{m}$-kg/hr) 1	2	Heat Capacity (C_{tf}-KJ/kg°C) 1	2	Heat Rate (q-KJ/hr) 1 Max.	1 Min.	2 Max.	2 Min.	Capacity (hr) At Max. Heat Rate CC/q 1	DC/q 2	At Min. Heat Rate CC/q 1	DC/q 2
62	133	153	1.012	1.002	4,510	1,180	4.680	1,340	5.0	4.8	19.3	16.8
63	135	152	1.016	1.003	4,600	1,200	4,650	1,330	5.0	4.9	19.0	17.1
				Average	4,560	1,190	4,670	1,340	5.0	4.9	19.2	17.0
59	115	134	1.014	1.002	3,910	1,020	4,100	1,170	5.9	5.6	22.5	19.7
60	117	130	1.012	1.002	3,970	1,040	3,970	1,140	5.8	6.1	22.3	21.4
61	114	129	1.013	1.002	3,870	1,010	3,940	1,130	5.8	5.9	22.4	20.6
				Average	3,920	1,020	4,000	1,150	5.8	5.9	22.4	20.6
64	99	113	1.012	1.002	3,360	880	3,450	990	6.8	7.4	26.1	22.8
65	82	94	1.013	1.001	2,780	730	2,870	820	8.3	7.6	31.5	26.7
66	83	96	1.009	1.003	2,810	730	2,940	840	8.7	7.6	33.4	26.8
				Average	2,800	730	2,910	830	8.5	7.6	32.5	26.8

1 = Charge

2 = Discharge

	T_{in}	T^{o}_{out}	T^{f}_{out}	ΔT	ΔT^{o}	ΔT^{f}
Charging (°C)	44.5	≈ 11	35.75	$T_{in}-T_{out}$	33.5	8.75
Discharging (°C)	9.5	≈ 40	18.25	$T_{out}-T_{in}$	30.5	8.75

the inlet temperature, since the difference of the inlet and outlet temperatures (ΔT) is the greatest. Similarly, the minimum useful charge (discharge) rate corresponds to the smallest temperature difference of the air streams observed at the end of the test time.

These maximum and minimum heat rates are tabulated for each run and plotted against the air flow rate in Figure 13. As expected, the heat rates decrease with decreasing air flow rate. The higher density of the cool air stream used for discharging results in a higher mass flow rate and hence, slightly higher heat rate curves for the discharging cycles.

For a given air flow rate, a nearly ideal latent heat storage unit would quickly decrease from its maximum heat rate to a constant heat rate for most of the test period, while the storage medium absorbed (evolved) its latent heat of fusion. Near the end of the test time the heat rate would again decrease quickly to finish at its minimum value. In actual practice a storage unit might operate between 10 and 90 percent of its storage capacity. This would maintain the heat rate at a fairly constant level, since charging (discharging) would operate almost exclusively on the latent heat of fusion. Note that the design rate for this particular size storage unit is set equal to the value corresponding to the minimum heat rate for a given air flow rate.

A storage capacity expressed in hours can be determined for charging (discharging) the storage unit at a constant heat rate. Such capacities were calculated and plotted against the air flow rate (Figure 14). These curves show the storage lifetime of the unit if total charging (discharging) occurred at the minimum or maximum heat rate. The actual charge (discharge) profiles, as shown earlier in Figure 9, fall between these hypothetical curves, since the actual heat rate varies from the maximum to the minimum values.

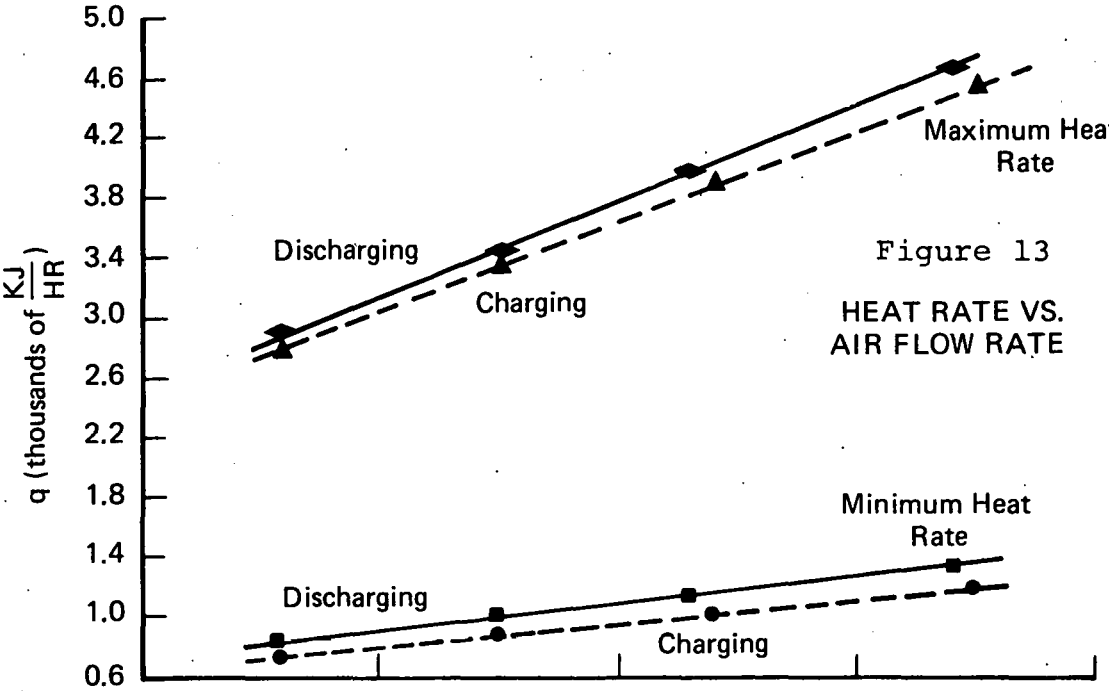

Figure 13

HEAT RATE VS.
AIR FLOW RATE

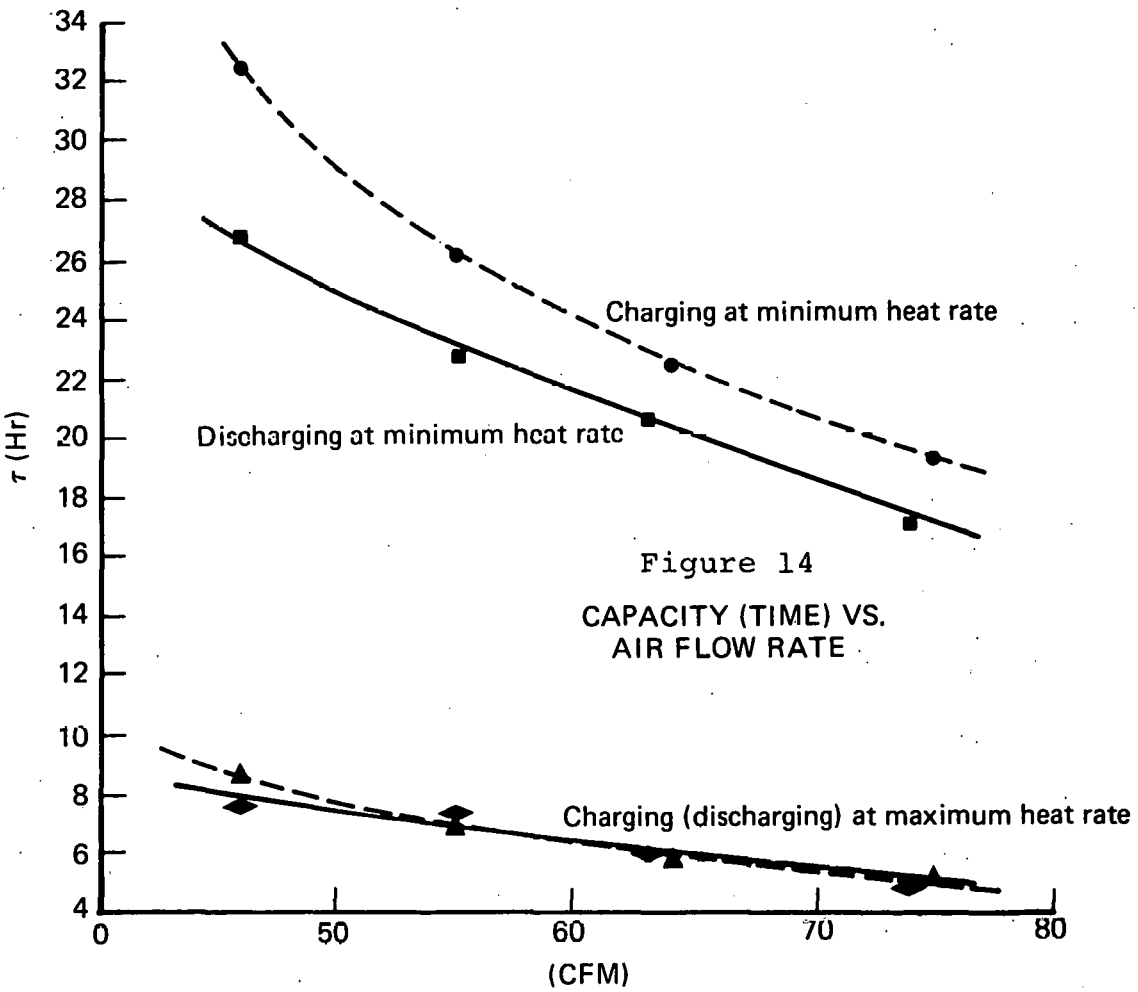

Figure 14

CAPACITY (TIME) VS.
AIR FLOW RATE

Nomenclature

C_{tf} = specific heat of transfer fluid - $\frac{CAL}{G°C}$

CC = charge capacity of thermal storage unit - KJ

DC = discharge capacity of thermal storage unit - KJ

L = heat loss rate - $\frac{KJ}{HR°C}$

$\dot{m}$ = mass flow rate of transfer fluid - $\frac{KG}{HR}$

ΔP = pressure differential across storage unit - in. H_2O

q = heat rate $\frac{KJ}{HR}$

Q = total heat - KJ

Q_{in} = total heat delivered to storage unit through transfer fluid - KJ

Q_{out} = total heat delivered by storage unit through transfer fluid - KJ

$\overline{T}_a$ = average ambient temperature - °C

T_{in} = temperature of transfer fluid entering storage unit - °C

T_{out} = temperature of transfer fluid leaving storage unit - °C

$\overline{T}_{unit}$ = average temperature of storage unit $(\frac{T_{in}+T_{out}}{2})$ - °C

ΔT = temperature difference of inlet and outlet $|T_{in}-T_{out}|$ - °C

τ = test time (hr)

τ_c = charging test time (hr)

τ_d = discharging test time (hr)

V. UTILIZATION ACTIVITY

We believe it is time to equip a demonstration building with a $CaCl_2 \cdot 6H_2O$ PCM storage unit. The heating system chosen is a tempered-water multiple heat pump system with liquid-cooled solar collectors. We are searching for a suitable building and suitable partners - architect, heat pump manufacturer, solar system supplier, contractors, etc.

We have contacted Penn State University and Ohio Agricultural R&D Center to suggest cooperative programs in utilizing encapsulated $CaCl_2 \cdot 6H_2O$ for heating greenhouses.

VI. PLANS

1. Initiate testing of magnesium nitrate hexahydrate in steel aerosol cans and start lifetime testing of this PCM/container combination.

2. Update storage unit computer model to fit calcium chloride hexahydrate results and perform sensitivity analysis of capacity to container diameter.

3. Fabricate pouches of R-2 retort film for encapsulation of magnesium nitrate hexahydrate/ammonium nitrate eutectic and start lifetime testing of the PCM/container combinaton.

4. Update economic analysis of thermal storage unit design.

5. Evaluate compatibility of storage unit design with various components of solar energy systems using TRNSYS computer simulation approach.

VII. CONCLUSIONS

Testing has been completed on $CaCl_2 \cdot 6H_2O$ encapsulated in polyethylene bottles in the storage test device. Good values were obtained for measured charge and discharge capacity, and a good energy balance was achieved. The capacities measured represent 90-98% (ave. 94%) of the theoretical capacity.

VIII. Report Distribution List

2 copies - Dr. Frederick H. Morse
U. S. Department of Energy
Heating and Cooling Branch
20 Massachusetts Avenue
Washington, D.C. 20545

2 copies - Dr. Henry H. Marvin
Division of Solar Energy
U. S. Department of Energy
20 Massachusetts Avenue
Washington, D.C. 20545

10 copies - Mr. Herbert W. Hoffman
Oak Ridge National Laboratory
P. O. Box X
Bldg. 9204-1, Mail Stop 3
Oak Ridge, Tennessee 37830

2 copies - Mr. A. H. Frost, Jr.
Contract Division, ORO
U. S. Department of Energy
P. O. Box E
Oak Ridge, Tennessee 37830

1 copy - Mr. Stewart Phillips
U. S. Department of Energy
P. O. Box E
Oak Ridge, Tennessee 37830

VIII. Report Distribution (continued)

Mr. John W. Leech
U. S. Department of Energy
20 Massachusetts Avenue
Washington, D.C. 20545

Mr. Charles J. Swet
U. S. Department of Energy
Division of Conservation Research & Technology
Washington, D.C. 20545

Mr. Harold G. Lorsch
The Franklin Institute
Research Laboratories
Twentieth and Parkway
Philadelphia, PA 19103

Miss Maria Telkes
University of Delaware
Institute of Energy Conversion
Newark, Delaware 19711

Mr. John A. Bailey
North Carolina State University
Raleigh, NC 27607

Dr. Adelbert T. Tweedie
General Electric Co.
Box 8555
Philadelphia, PA 19101

Mr. Richard L. Merriam
A. D. Little, Inc.
20 Acorn Park
Cambridge, MA 02140

Mr. Guy Ervin
Atomics International Division
Rockwell International
8900 DeSoto Avenue
Canoga Park, CA 91304

Mr. Dieter Gruen
Argonne National Laboratory
Chemical Division
9700 S. Cass Avenue
Argonne, IL 60439

VIII. Report Distribution List (continued)

Mr. Rudy Duscha
Mail Stop 500-318
National Aeronautics and Space Agency
Lewis Laboratory
21000 Brookpark Road
Cleveland, OH 44135

Mr. Frank Salzano
Head Storage & Conversion Division
Bldg. 475
Brookhaven Nat. Lab.
Upton, NY 11973

Mr. J. Douglas Balcomb/Dr. H. R. Herr
Solar Energy Group
Los Alamos Scientific Lab.
P. O. Box 1663
Los Alamos, New Mexico 87544

Mr. Allan Michaels
Argonne National Laboratory
9700 South Cass Avenue
Argonne, Illinois 60439

Dr. Stephen L. Sargent
U. S. Department of Energy
Research & Development Branch
Division of Solar Energy
20 Massachusetts Avenue
Washington, D. C. 20545

Dr. D. D. Edie
Chem. Engr. Dept.
Clemson University
Clemson, South Carolina 29631

Mr. J. L. Eichelberger
Senior Research Chemist
Pennwalt Corporation
900 First Avenue
King of Prussia, Pennsylvania 19406

Dr. L. G. Marianowski
3424 S. State St.
Institute of Gas Technology
Chicago, Illinois 60616

VIII. Report Distribution List (continued)

Dr. C. Ernest Birchenall
University of Delaware
Department of Chemical Engineering
Newark, Delaware 19711

Dr. Day Chahroudi
Suntek
506 Tamal Plaza
Corte Madiera, CA 94925

Dr. Kenneth Kauffman
Franklin Institute
20th and Race Streets
Philadelphia, PA 19103

Dr. William H. Horn
Brookhaven National Laboratory
Building 526
Upton, NY 11973